HHS Public Access

Author manuscript

J Steroid Biochem Mol Biol. Author manuscript; available in PMC 2022 April 30.

Published in final edited form as:

J Steroid Biochem Mol Biol. 2017 October ; 173: 185–193. doi:10.1016/j.jsbmb.2017.02.005.

Class 3 semaphorins are transcriptionally regulated by $1,25(OH)_2D_3$ in osteoblasts

Jussi Ryynänen[a], **Carsten Kriebitzsch**[a], **Mark B. Meyer**[b], **Iris Janssens**[a], **J. Wesley Pike**[b], **Lieve Verlinden**[a,1], **Annemieke Verstuyf**[a,*,1]

[a]Clinical and Experimental Endocrinology, KULeuven, Herestraat 49, Bus 902, 3000 Leuven, Belgium

[b]Department of Biochemistry, University of Wisconsin-Madison, Madison, WI, 53706, USA

Abstract

The vitamin D endocrine system is essential for calcium metabolism and skeletal integrity. 1,25-dihydroxyvitamin D_3 [$1,25(OH)_2D_3$] regulates bone mineral homeostasis and acts directly on osteoblasts. In the present study we characterized the transcriptional regulation of the class 3 semaphorin (*Sema3*) gene family by $1,25(OH)_2D_3$ in osteoblastic cells. Class 3 semaphorins are secreted proteins that regulate cell growth, morphology and migration, and were recently shown to be involved in bone homeostasis. In ST2, MC3T3-E1 and primary calvarial osteoblast cell cultures we found that all members of the *Sema3* gene family were expressed, and that *Sema3e* and *Sema3f* were the most strongly induced $1,25(OH)_2D_3$ target genes among the studied cell types. In addition, transcription of *Sema3b* and *Sema3c* was upregulated, whereas *Sema3d* and *Sema3g* was downregulated by $1,25(OH)_2D_3$ in different osteoblastic cells. Chromatin immunoprecipitation analysis linked to DNA sequencing (ChIP-seq analysis) revealed the presence of the vitamin D receptor at multiple genomic loci in the proximity of *Sema3* genes, demonstrating that the genes are primary $1,25(OH)_2D_3$ targets. Furthermore, we showed that recombinant SEMA3E and SEMA3F protein were able to inhibit osteoblast proliferation. However, recombinant SEMA3s did not affect ST2 cell migration. The expression of class 3 semaphorins in osteoblasts together with their regulation by $1,25(OH)_2D_3$ suggests that these genes, involved in the regulation of bone homeostasis, are additional mediators for $1,25(OH)_2D_3$ signaling in osteoblasts.

Keywords

Vitamin D; Vitamin d receptor; Semaphorin; Osteoblast; Transcription; Gene expression regulation

*Corresponding author. mieke.verstuyf@med.kuleuven.be (A. Verstuyf).

[1]These authors contributed equally to this work.

Appendix A. Supplementary data

Supplementary data associated with this article can be found, in the online version, at http://dx.doi.org/10.1016/j.jsbmb.2017.02.005.

1. Introduction

The semaphorin (SEMA) superfamily consists of a large number of cell surface and secreted glycoproteins that are involved in axonal growth cone guidance, cell migration, cardiogenesis, angiogenesis, tumor growth and immune responses [1–5]. The class 3 semaphorin (SEMA3) family consists of 7 members (SEMA3A through 3G) and are the only secreted semaphorins in vertebrates [1]. Except for SEMA3E, which directly binds the plexin (PLXN) D1 receptor [6], SEMA3 proteins first bind to neuropilin (NRP) receptors. After NRP binding, PLXNA co-receptors are recruited that serve as the primary receptors that transduce the signal to the cytoplasm, while NRPs stabilize the receptor complex [7]. The composition of the NRP/PLXN receptor complex determines the binding affinity of the SEMA3 ligands to the NRP receptors and may depend on cell or tissue type [8], allowing cell-type specific signaling.

Lately, semaphorins have gained attention for their involvement in normal bone homeostasis and bone pathology [9–11]. Semaphorin molecules of different classes are widely expressed in bone cells and SEMA3s may either promote (SEMA3B) or inhibit (SEMA3A, SEMA3E) osteoclast formation [12]. Moreover, SEMA3A is also able to promote osteoblastic bone formation [9]. These studies suggest that semaphorin signaling participates in the complex cross-talk between osteoblasts and osteoclasts, which indicates that they may have therapeutic potential for the treatment of bone disorders.

The classical role of 1α,25-dihydroxyvitamin D_3 [1,25$(OH)_2D_3$], the most biologically active vitamin D_3 metabolite, is to maintain adequate serum levels of calcium and phosphate by stimulating calcium absorption in the intestine, by increasing reabsorption of calcium and phosphate in the kidney, and by releasing calcium and phosphate from skeletal stores [13]. Although 1,25$(OH)_2D_3$ has direct effects on bone formation and osteoblasts, its exact role in bone cells has yet to be completely unraveled [14]. 1,25$(OH)_2D_3$ exerts its functions through the vitamin D receptor (VDR), a ligand-activated transcription factor that belongs to the nuclear receptor superfamily. To directly regulate the transcription of primary 1,25 $(OH)_2D_3$ target genes, ligand-activated VDR forms a heterodimer with the retinoid X receptor (RXR) and binds DNA at specific vitamin D responsive elements (VDREs), preferentially the DR3-type VDREs that are formed by direct repeats of two hexameric core binding sequences spaced by three nucleotides [15,16]. Interestingly, different studies have illustrated that 1,25$(OH)_2D_3$ induces the expression of several class 3 semaphorins. Indeed, *Sema3b* as well as *Sema3e* are transcriptionally upregulated by 1,25 $(OH)_2D_3$ in osteoblasts [17,18]. Moreover, 1,25$(OH)_2D_3$ upregulates *Sema3b* in prostate cancer cells [19], and induces SEMA3B and SEMA3F protein levels in malignant endometrial cancer cells [20]. However, none of these studies deciphered whether these *Sema3* genes are primary targets of 1,25$(OH)_2D_3$.

The findings that 1,25$(OH)_2D_3$ induces expression levels of different *Sema3* ligands prompted us to investigate the transcriptional regulation of all seven members of the *Sema3* family genes in osteoblastic cell cultures after treatment with 1,25$(OH)_2D_3$. In addition, we demonstrated by chromatin immunoprecipitation sequencing (ChIP-seq) analyses a number of active VDR binding sites across the genomic loci for the *Sema3* genes. Finally, we

attempted to decipher possible roles of recombinant SEMA3s in osteoblast proliferation and migration.

2. Materials and methods

2.1. Cell culture

MC3T3-E1 pre-osteoblast and bone marrow-derived stromal ST2 cells (both from Riken Cell Bank, Japan) were maintained in Minimum Essential Medium alpha with GlutaMAX (α-MEM, Gibco) supplemented with 10% FBS, 100 units/ml penicillin and 100 μg/ml streptomycin. Primary calvarial osteoblasts were isolated from newborn C57BL/6 mice (Harlan Laboratories) as described previously [21]. The day after seeding, treatment with vehicle (PBS or ethanol), with recombinant SEMA3A, 3B, 3C, 3E, or 3F (R&D Systems), or with 10^{-8} M $1,25(OH)_2D_3$ (Sigma-Aldrich) was started. The final concentration of ethanol in the medium was lower than 0.001%.

Gene expression during *in vitro* osteoblastic mineralization was assessed by culturing calvarial osteoblasts until confluency, and supplementing the culture medium with 50 μg/ml ascorbic acid (Sigma-Aldrich) and 10 mM β-glycerophosphate (Sigma-Aldrich). At days 13 and 20 after the switch to osteogenic medium, cultures were incubated with vehicle or 10^{-8} M $1,25(OH)_2D_3$ for 24 h.

To measure cellular proliferation, ST2 and MC3T3-E1 cells were incubated for 72 h with recombinant SEMA3A, 3B, 3C, 3E, or 3F (R&D Systems) and 1 μCi [^{3}H]thymidine (specific activity of 2 Ci/mmol, PerkinElmer) was added. After an additional 4 h incubation period [^{3}H]thymidine incorporation into cells was measured as described previously [22].

2.2. RNA extraction, cDNA synthesis and qPCR

Total RNA was isolated, cDNA prepared with Oligo $d(T)_{16}$ primers (Invitrogen), and quantitative real-time PCR (qPCR) reactions performed using 1/10 diluted cDNA templates with the Fast SYBR Green Master Mix (Applied Biosystems) or the TaqMan Fast Universal PCR Master Mix (Applied Biosystems) as described previously [22]. To obtain relative gene expression levels, the $2^{-\Delta Ct}$ method was used and the reference gene β-actin was used to normalize the gene expression.

2.3. Chromatin immunoprecipitation (ChIP) and ChIP-seq analysis

ChIP-seq analyses were previously performed in MC3T3-E1 cells (GSE51515 and GSE41955) [23,24]. Tag density for each factor was normalized to 10^7 tags and data normalized to input were displayed using the UCSC genome browser (http://genome.ucsc.edu/) [25], and is based on the Build 37 assembly (mm9) by the National Center for Biotechnology Information (NCBI) and the Mouse Genome Sequencing Consortium. ChIP-qPCR experiments using anti-VDR (sc-1008, Santa Cruz), anti-RXR (sc-774, Santa Cruz) and anti-tetra-acetylated histone H4 (06–866, Millipore) were performed with MC3T3-E1 cells treated for 3 h with 10^{-7} M $1,25(OH)_2D_3$ as described previously [23]. Cell lysates used in the ChIP-qPCR experiments were from three independent experiments and results were normalized with respect to input samples. The

specificity of receptor binding data by ChIP was confirmed by unspecific negative control region, where no VDR/RXR binding was observed according to ChIP-seq.

2.4. Transient transfection assays

Genomic DNA fragments (mm9) of *Sema3b* (chr9: 107,507,703–107,508,041; 339 bp in size) and *Sema3f* (chr9: 107,605,724–107,606,022; 299 bp in size) were cloned in a pGL3-Basic luciferase reporter vector (Promega). Vectors, in which 4 nucleotides from the DR3-type VDREs present in these genomic fragments were mutated, were prepared with the QuickChange II Site-Directed Mutagenesis kit (Stratagene). Exponentially growing MC3T3-E1 cells were transfected, stimulated following day with $1,25(OH)_2D_3$ (10^{-8} M) or vehicle, and subjected to luciferase activity assessment as described previously [26].

2.5. Scratch wound cell migration assay

Cell migration was analyzed in ST2 cells with the IncuCyte ZOOM Scratch Wound assay (Essen BioScience). Cells were grown overnight to form sub-confluent monolayers and treated for 2 h with recombinant SEMA3A, 3B, 3C, 3E, or 3F before 700–800 μm wide scratch wounds were prepared for each well with a 96-pin WoundMaker (Essen BioScience). The wound recovery was monitored every two hours by the IncuCyte ZOOM live cell imaging system and the data were analyzed with software version 2015A. A minimum of 12 replicate treatments per experiment was performed.

Data for each experiment were further analyzed as relative wound densities (RWD) over time. RWD (%) is a measure of the percentage change in relative spatial cell density in the initial wound area over the cell density outside the wound at every time point. RWD values as a function of time were plotted in a line chart, and area under the curve (AUC) was determined for each individual wound separately to obtain a comparable measure for cell migration kinetics. AUC was determined from RWD data obtained during 36 h of wound healing, as illustrated in Fig. S1, where approximately 75–85% RWD was reached and RWD still increased linearly over time (Fig. S1B).

2.6. Statistical analysis

The results are expressed as the mean and standard deviation. Two-tailed Student's *t*-tests of sample means, and one sample *t*-tests using log-transformed values of fold change data, were carried out to detect significant differences. The applied statistical tests are indicated in the figure legends. $p < 0.05$ was accepted as significant.

3. Results

3.1. $1,25(OH)_2D_3$ induced the transcription of different semaphorin 3 family members

In order to get an overview of osteoblastic gene expression of the different members of class 3 semaphorins, relative basal mRNA expression levels were analyzed by qPCR in the ST2 bone marrow-derived stromal cell line, in the MC3T3-E1 mouse pre-osteoblast cell line, and in cultures of primary calvarial osteoblasts (Fig. 1). Expression profiling revealed that all 7 genes were expressed in the studied cell types with *Sema3a*, *3c*, *3e* and *3f* being the most abundantly expressed in all investigated cell types. The expression pattern of the *Sema3*

genes was rather similar among the studied cell types, with the exception of *Sema3d*, which was only weakly expressed in ST2 and MC3T3-E1 cells, but rather abundantly expressed in primary calvarial osteoblasts.

When these cells were stimulated with $1,25(OH)_2D_3$ for 6 and 24 h, we observed that transcript levels of four semaphorin 3 family members, *Sema3b*, *3c*, *3e* and *3f*, were significantly induced in at least 2 cell types (Fig. 2). Transcriptional upregulation of *Sema3e* and *3f* by $1,25(OH)_2D_3$ was apparent after a 6 h incubation period in ST2 and MC3T3-E1 cells (Fig. 2A and B), and was observed at 24 h after stimulation in all investigated cell cultures (Fig. 2A, B, C, and D). Interestingly, even though their basal expression levels were high, *Sema3e and 3f* were the most inducible semaphorin 3 family genes in response to a 24 h treatment with $1,25(OH)_2D_3$ in all cell types, showing 9.1 and 3.5, 8.0 and 4.0, and 1.5 and 2.8 −fold inductions in ST2, MC3T3-E1 and calvarial osteoblast cells, respectively. Additionally, the induction of the genes was sustained for at least 72 h after stimulation (data not shown). Furthermore, the genes *Sema3b* and *3c* were induced in both ST2 and MC3T3-E1 cells after a 24 h incubation period with $1,25(OH)_2D_3$ demonstrating significant, but weaker and delayed upregulation compared to that of *Sema3e* and *3f* (Fig. 2A and B). Additionally, expression of S*ema3g* and *Sema3d* was regulated in a cell type-specific manner. Indeed, *Sema3g* expression was significantly downregulated in MC3T3-E1 cells at both measured time points (Fig. 2B), whereas *Sema3d* showed prominent downregulation in calvarial osteoblasts (Fig. 2C).

In summary, all semaphorin 3 family members were expressed in the osteoblastic cells we examined. The *Sema3e* and *3f* genes were strongly upregulated $1,25(OH)_2D_3$ targets in osteoblastic cells, while the *Sema3b* and *3c* genes responded to $1,25(OH)_2D_3$ only in ST2 and MC3T3-E1 cells, and *Sema3d* only in primary osteoblasts.

3.2. Sema3d, 3e *and* 3f *were transcriptionally regulated by 1,25 $(OH)_2D_3$ in primary mineralizing osteoblast cultures*

Subsequently, the effect of $1,25(OH)_2D_3$ on the expression of *Sema3* family members was investigated *in vitro* during osteogenic differentiation of primary calvarial osteoblasts. mRNA was isolated during early and late mineralization, days 14 and 21, respectively. In both studied time points, transcription of both *Sema3e* and *3f* showed prominent induction by $1,25(OH)_2D_3$ when mineralizing cultures were subjected to a short 24 h incubation period with $1,25\ (OH)_2D_3$ (Fig. 2D). The magnitude of the inductions was similar at both mineralization phases (3–3.2 −fold for both genes), which was slightly stronger for *Sema3e* than that observed in non-mineralized osteoblasts (Fig. 2C). In addition, transcript levels of *Sema3d* were significantly reduced after treatment with $1,25\ (OH)_2D_3$, which was also observed before mineralization. No induction of *Sema3b* was observed by $1,25(OH)_2D_3$ during the mineralization process (Fig. 2D) whereas a modest downregulation of *Sema3c* expression was demonstrated.

Taken together, the upregulation of the *Sema3e* and *Sema3f* genes and the downregulation of *Sema3d* by $1,25(OH)_2D_3$ was observed during mineralization of primary calvarial osteoblasts.

3.3. *ChIP-seq experiments revealed direct binding of VDR and RXR to the genomic regions of the* Sema3 *genes*

Because the induction of *Sema3* genes by 1,25$(OH)_2D_3$ was observed in osteoblastic cell cultures, we used ChIP-seq analyses of VDR and RXR binding and selected histone modifications in MC3T3-E1 cells to demonstrate the basis of *Sema3* regulation by VDR in more detail. All observed VDR peaks co-localized with RXR peaks demonstrating the presence of VDR/RXR heterodimers at these sites (Fig. 3). Intronic VDR/RXR peaks were present at two and three sites of the *Sema3b* and *3f* genes, respectively (Fig. 3A). In the larger genomic region spanning 20 kb downstream from *Sema3b* to 35 kb upstream from *Sema3f* genes, which contains eight intervening and adjacent genes, the presence of at least 14 VDR/RXR peaks was demonstrated with the strongest and most inducible peaks near the *Sema3b* and *3f* transcription start site (TSS). In contrast, a ten-fold larger genomic region covering the genes *Sema3d*, *Sema3a* and *Sema3e* contains only one intervening gene, but demonstrated at least 15 peaks for VDR and RXR binding (Fig. 3B). Interestingly in this genomic locus, VDR peaks focused between the *Sema3d* and *Sema3e* genes, since no VDR/RXR peaks were observed within 500 kb down- or upstream from the displayed region (data not shown). Similarly, ChIP-seq data revealed clustered VDR/RXR binding around the *Sema3c* (Fig. 3C) and *Sema3g* (Fig. 3D) genes, both genes being 1,25 $(OH)_2D_3$ targets in MC3T3-E1 cells.

The specific histone modifications, H4K5 and H3K9 acetylation (H4K5ac and H3K9ac, enriched at active chromatin [27]), and H3K4 mono-methylation (H3K4me1, enriched across enhancers [27]) showed a remarkably similar landscape amongst most of the VDR/RXR binding sites (Fig. 3). With no exceptions, VDR/RXR binding sites were aligned with H4K5ac peaks that, in general, demonstrate accessible chromatin structures. In addition, H4K5ac levels showed some response to 1,25$(OH)_2D_3$ treatment displaying both increase and decrease of acetylation at different VDR binding sites. H3K9ac peaks aligned with H4K5ac peaks. However, the magnitude of H3K9ac peaks showed great peak-to-peak variation. With few exceptions all VDR/RXR binding sites aligned with strong H3K4me1 levels demonstrating enhancer activity around the VDR/RXR heterodimer. Moreover, VDR binding sites at all studied regions generally aligned within valleys of distinct peak-valley-peak patterns created by histone modification levels (For detailed view, the reader is referred to the original ChIP-seq data tracks). This pattern highlights nucleosome free regions that are accessible for additional regulatory factors, and are enriched within enhancers in active state [28].

Subsequently, we performed ChIP-qPCR experiments with selected VDR binding sites at the *Sema3b* and *Sema3f* loci based upon their highly induced VDR binding and proximity of the respective gene TSS (locations indicated at Fig. 3). For both sites, we confirmed the increase in VDR and RXR binding after incubation with 1,25$(OH)_2D_3$ (Fig. 4A and B). Both VDR binding sites carried a DR3-type VDRE sequence for direct VDR binding and demonstrated a significant increase in acetylation levels (AcH4) (Fig. 4C). The specificity of receptor binding was confirmed by qPCR of a negative control region that is located at the second intron of the *Slc38a3* gene between the genes *Sema3b* and *Sema3f* (Fig. 3, 4A and 4B). No VDR or RXR binding was seen on the negative region. In order to

further confirm the functionality of the studied VDR binding sites of *Sema3b* and *Sema3f*, both DR3-type VDREs were cloned in luciferase reporter vectors and used in transient transfection experiments (Fig. 4D). Luciferase activities of reporter vectors with the genomic fragments of *Sema3b* and *3f* were significantly induced when transfected MC3T3-E1 cells were incubated for 24 h with 1,25$(OH)_2D_3$ (4.2 and 3.8 −fold, respectively). Subsequently, the DR3-type binding sites were mutated before transfection, to prevent VDR binding, and luciferase activity was evaluated in 1,25 $(OH)_2D_3$-or vehicle-treated cells. Interestingly, the induction of luciferase activity by 1,25$(OH)_2D_3$ was completely abolished with the mutated reporter constructs, indicating that the suspected VDR binding sites were responsible for the transactivation of the reporter constructs.

In summary, ChIP experiments revealed around all seven *Sema3* genes numerous intronic and intergenic VDR/RXR heterodimer binding sites that were co-localized with histone markers for active chromatin structure and enhancer activity. Ligand-inducible VDR and RXR binding was confirmed and a prominent increase in histone H4 acetylation was shown for both studied VDR sites in ChIP-qPCR experiments. In addition, the functionality of the VDR binding sites was confirmed in transient transfection assays.

3.4. Recombinant SEMA3E and SEMA3F decreased cell proliferation

In order to evaluate the possible function of the VDR-regulated class 3 semaphorins, we investigated whether recombinant semaphorin 3 proteins affected cell proliferation. ST2 and MC3T3-E1 cells were cultured for 3 days in the presence of recombinant SEMA3 proteins and proliferation was measured by a [^{3}H]thymidine incorporation assay. Incubation with recombinant SEMA3E as well as SEMA3F led to a small, but significant, reduction of cell proliferation in both cell lines (Fig. 5).

3.5. Recombinant semaphorin 3 proteins did not affect ST2 cell migration

Class 3 semaphorins are known modulator of cell migration in different tissues [29]. Therefore, we performed scratch wound assays in ST2 cells that were treated with recombinant SEMA3 proteins prior to scratching the wound. A minor, but significant, inhibition of ST2 cell migration after incubation with SEMA3F was observed (Fig. 6). The other class 3 semaphorin family members did not alter the wound healing speed.

In order to further investigate the role of SEMA3 in pre-osteoblasts, we treated exponentially growing ST2 cells for 72 h with recombinant SEMA3 proteins (600 ng/ml), and measured the mRNA inductions of osteoblast lineage genes (runt-related transcription factor 2, osteopontin and osteocalcin) and of osteoclastic marker receptor activator of nuclear factor κB ligand (RANKL, encoded by the *Tnfsf11* gene). We saw no changes in the expression levels of the studied genes in response to the treatment (data not shown).

4. Discussion

Semaphorins were first identified as molecules involved in axonal guidance during the development of the nervous system but are now recognized as crucial regulators of homeostasis over a wide range of organ systems. SEMA3s in particular affect cell growth, survival and migration in neuronal as well as non-neuronal tissues [3,5], and there is an

increasing body of evidence that SEMA3 signaling is present in bone and may affect bone homeostasis [12]. In order to investigate the effect of $1,25(OH)_2D_3$ on *Sema3* gene expression at distinct stages of osteoblast differentiation, we used ST2 cells derived from mouse bone marrow, which have stem cell characteristics and can be differentiated into osteoblasts [30], MC3T3-E1 pre-osteoblasts, and both unmineralized and mineralizing primary calvarial osteoblasts. Our study demonstrated that all members of the *Sema3* family were expressed in the three osteoblastic cell types and that the basal expression patterns of *Sema3* genes in these cells were remarkably similar. We showed that the expression of six different *Sema3* family members (*Sema3b*, *3c*, *3d*, *3e*, *3f* and *3g*) was altered by $1,25(OH)_2D_3$ in at least one osteoblastic cell type, suggesting that these molecules are additional mediators for the effects of $1,25(OH)_2D_3$ on osteoblasts. Of interest, transcript levels of *Sema3e* and *3f* were rapidly and robustly induced by $1,25(OH)_2D_3$ (within 6 h after treatment), not only in osteoblastic cell lines but also in both unmineralized and mineralizing primary calvarial osteoblasts, suggesting that *Sema3e* and *Sema3f* are conserved 1,25 $(OH)_2D_3$ targets over the different osteoblastic cell types. Since these strongly inducible genes were also highly expressed in these cells, *Sema3e* and *Sema3f* may be important mediators of the 1,25 $(OH)_2D_3$ signaling in osteoblasts. Consistent with our results, the induction of *Sema3e* in response to $1,25(OH)_2D_3$ was previously reported in non-differentiated calvarial osteoblasts [18]. Furthermore, transcript levels of *Sema3b* and *Sema3c* were increased after $1,25(OH)_2D_3$ treatment, but only in the ST2 and MC3T3-E1 cell lines and not in calvarial osteoblasts. The induction of *Sema3b* in response to $1,25(OH)_2D_3$ in ST2 cells was previously reported by Sutton et al. [17]. However, in their study a modest induction of *Sema3b* by $1,25(OH)_2D_3$ was observed also in mineralizing primary calvarial osteoblasts. Downregulation of transcript levels of *Sema3g* by $1,25(OH)_2D_3$ was only observed in MC3T3-E1 cells whereas *Sema3d* mRNA levels were only downregulated in calvarial osteoblasts, both in unmineralized and mineralizing cultures. The latter corresponds with a study performed in mouse calvarial osteoblasts, where a trend for reduction in *Sema3d* transcripts in response to $1,25(OH)_2D_3$ is observed [18]. While we demonstrated that all other members of the *Sema3* gene family were regulated by $1,25(OH)_2D_3$ in osteoblastic cells, we did not observe any evidence that *Sema3a* was a $1,25(OH)_2D_3$ target gene in these cells, which is consistent with a previous report in osteoblasts [18].

To investigate whether the $1,25(OH)_2D_3$-induced *Sema3* genes were directly regulated by VDR, we utilized ChIP-seq data from MC3T3-E1 cells to demonstrate VDR/RXR binding and presence of histone modifications indicating active enhancers at the genomic regions around the *Sema3* genes. We observed the presence of strongly inducible VDR/RXR heterodimers accompanied by accessible chromatin architecture (H4K5ac and H3K9ac) and enhancer activity (H3K4me1) at several intronic and intergenic locations of all transcriptionally upregulated *Sema3* genes (*Sema3b*, *3f*, *3e* and *3c*) and the downregulated *Sema3g* gene. Our observations suggest that these genes are indeed primary $1,25(OH)_2D_3$ targets and that each gene is most likely regulated by multiple VDR binding sites in osteoblastic cells. For example, the *Sema3c* locus demonstrated a group of ligand-induced VDR peaks positioned around the end of the *Sema3c* gene. Accordingly, the VDR peaks aligned with highly induced RXR peaks and showed open chromatin structure in

combination with enhancer activity as defined by the histone modifications, which suggest that these VDR binding sites are activated by $1,25(OH)_2D_3$ stimulation and responsible for the *Sema3c* transactivation.

Interestingly, non-responsive *Sema3d* and *Sema3a* in this cell line also showed numerous prominent VDR/RXR binding sites clustered around these two genes. Although the histone modification landscape was generally similar amongst the VDR binding sites, the underlying mechanisms for the observed ineffective VDR binding may involve the small differences observed in histone modification responses to $1,25(OH)_2D_3$ treatment. For example, all the H4K5ac peaks upstream of *Sema3b* TSS showed some degree of induction after $1,25(OH)_2D_3$ treatment. In contrast, at many VDR sites of non-responsive *Sema3d* and *Sema3a* acetylation levels were unchanged or reduced. In accordance, a very strong VDR peak between the genes lacked an H3K4me1 peak. We speculate that this may suggest inactivity of the VDR site. It is also possible that the lack of response to $1,25(OH)_2D_3$ may be due to the presence of silencing marks such as H3K27me3 or H3K9me3 not evaluated here or perhaps the absence of additional unknown transcription factors. Nevertheless, these data suggest that the epigenetic histone status of the enhancers to which the VDR is bound likely contributes to the receptor's transactivation ability at these genes, and may also explain why the non-responding *Sema3d* gene in MC3T3-E1 cell line can respond to treatment in primary osteoblasts. The similarity of *Sema3d* and *Sema3a* chromatin landscape with multiple VDR/RXR binding sites raises the question as to whether *Sema3a* would respond to $1,25(OH)_2D_3$ in osteoblastic cells in an alternative epigenetic state.

To further analyze the observations from ChIP-seq data, we focused on the genomic region containing the *Sema3b* and *Sema3f* genes as an example, and selected two highly inducible VDR peaks at the proximity of the respective gene TSS for our ChIP-qPCR and transfection assays. ChIP-qPCR results confirmed the $1,25(OH)_2D_3$-inducible VDR/RXR binding to both sites and demonstrated prominent chromatin opening during VDR activation. In addition, *Sema3f* region showed in both absence and presence of ligand stronger VDR binding than that at *Sema3b*, which is in line with the earlier and more prominent mRNA inductions of *Sema3f*. Subsequent *in silico* screening revealed the presence of putative DR3-type VDREs in VDR/RXR-bound regions. Transient transfection experiments combined with site directed mutagenesis demonstrated that the *in silico* identified DR3-type VDREs were indeed functional. Interestingly, increased protein levels of SEMA3B and SEMA3F in response to $1,25(OH)_2D_3$ treatment is observed in endometrial cancer cells [20], which demonstrates that these primary target genes can be regulated by $1,25(OH)_2D_3$ in other tissues.

Although the definite physiological outcome of the $1,25\ (OH)_2D_3$-inducible *Sema3* gene expression remains obscure, these proteins are suggested to be involved in the communication between osteoblasts and osteoclasts [18,31]. Expression of *Sema3f*, but also that of *Sema3a* and *Sema6b*, was reduced in ST2 cells in which *Runx2*, a master regulator of osteoblast differentiation, is overexpressed [31]. Overexpression of *Runx2* in ST2 cells results in an enhanced differentiation of co-cultured pre-osteoclasts and the authors propose that the downregulation of *Sema3f*, *Sema3a* and *Sema6b* is involved in *Runx2*-driven osteoclastogenesis [31]. In addition, loss of *Nrp2*, the main receptor for SEMA3F, leads

to bone loss that is accompanied by an enhanced osteoclast number and a reduced osteoblast count [32]. Interestingly, SEMA3E is also suggested to inhibit osteoclastogenesis, as an inhibitory effect of recombinant SEMA3E on osteoclast formation is reported in mouse marrow hematopoietic cells that were cultured in the presence of macrophage colony stimulating factor and RANKL [18]. These studies suggest that upregulation of *Sema3e* and *Sema3f* may inhibit osteoclast formation. In contrast, osteoblast-derived SEMA3B is demonstrated to promote *in vivo* osteoclastogenesis, leading to osteopenia when overexpressed [17]. However, recent observations that osteoblastic SEMA3B is suppressed in osteoporotic mice and that SEMA3B may promote *in vitro* osteoblast differentiation [33], suggest a more complex role of this protein in bone homeostasis. Furthermore, reduced expression of *Sema3d* in cortical bone in a mouse model for hypophosphatemic rickets is reported suggesting that SEMA3D may be associated with mineralization defects observed in the osteoblasts of these mice [34]. However, our observation that SEMA3 treated ST2 cells did not change the expression of early osteoblastic markers or *Tnfsf11* gene suggests that SEMA3s are not involved in osteoblast differentiation or in the regulation of RANKL.

SEMA3s are demonstrated to modulate cell migration and chemotaxis in a variety of tissues by their capabilities to influence cytoskeletal organization and cell adhesion [29,35,36]. However, we did not observe major effects of recombinant semaphorins on cell migration in ST2 cells. Our findings are inconsistent with those reported in mouse calvarial osteoblasts, where an inhibitory effect of recombinant SEMA3E protein on osteoblast migration is observed [18]. In our cellular model, the faint reduction in wound healing after SEMA3F treatment may be explained by a reduction in cell proliferation. Indeed, we demonstrated that recombinant SEMA3E and SEMA3F were able to inhibit osteoblast proliferation, which may suggest that *Sema3e* and *Sema3f* are involved in the antiproliferative effects of $1,25(OH)_2D_3$.

In conclusion, we showed that $1,25(OH)_2D_3$ directly controls the transcriptional regulation of members of the *Sema3* gene family. In addition, we showed that *Sema3b*, *Sema3c*, *Sema3e* and *Sema3f* are upregulated and *Sema3d* and *sema3g* are downregulated 1,25 $(OH)_2D_3$ target genes within osteoblastic cells, providing more evidence for the involvement of $1,25(OH)_2D_3$ in the osteoblastic signaling.

Supplementary Material

Refer to Web version on PubMed Central for supplementary material.

Acknowledgements

We thank Ine Beullens, Biauw Keng Tan and Mark Van Camp for excellent technical assistance. This work was supported by grants from the Fund for Scientific Research [FWO G.OA17.14N]; the KU Leuven [GOA/14/010]; the Orion Research Foundation (to J.R.); the Osk. Huttunen Foundation (to J.R.); and, in part, by the National Institutes of Health grant R01-DK072281 (to J.W.P.).

Abbreviations:

$1,25(OH)_2D_3$	1,25 dihydroxyvitamin D_3

AUC	area under the curve
ChIP	chromatin immunoprecipitation
ChIP-seq	ChIP sequencing
NRP	neuropilin
PLXN	plexin
RWD	relative wound density
RXR	retinoid X receptor
Sema3	class 3 semaphorin
TSS	transcription start site
VDR	vitamin D receptor
VDRE	vitamin D responsive element

References

[1]. Castellani V, Rougon G, Control of semaphorin signaling, Curr. Opin. Neurobiol. 12 (5) (2002) 532–541. [PubMed: 12367632]

[2]. Kruger RP, Aurandt J, Guan KL, Semaphorins command cells to move, Nat. Rev. Mol. Cell Biol. 6 (10) (2005) 789–800. [PubMed: 16314868]

[3]. Gaur P, Bielenberg DR, Samuel S, Bose D, Zhou Y, Gray MJ, Dallas NA, Fan F, Xia L, Lu J, Ellis LM, Role of class 3 semaphorins and their receptors in tumor growth and angiogenesis, Clin. Cancer Res. 15 (22) (2009) 6763–6770. [PubMed: 19887479]

[4]. Takamatsu H, Okuno T, Kumanogoh A, Regulation of immune cell responses by semaphorins and their receptors, Cell Mol. Immunol. 7 (2) (2010) 83–88.

[5]. Epstein JA, Aghajanian H, Singh MK, Semaphorin signaling in cardiovascular development, Cell Metab. 21 (2) (2015) 163–173. [PubMed: 25651171]

[6]. Oh WJ, Gu C, The role and mechanism-of-action of Sema3E and Plexin-D1 in vascular and neural development, Semin. Cell Dev. Biol. 24 (3) (2013) 156–162. [PubMed: 23270617]

[7]. Janssen BJ, Malinauskas T, Weir GA, Cader MZ, Siebold C, Jones EY, Neuropilins lock secreted semaphorins onto plexins in a ternary signaling complex, Nat. Struct. Mol. Biol. 19 (12) (2012) 1293–1299. [PubMed: 23104057]

[8]. Sharma A, Verhaagen J, Harvey AR, Receptor complexes for each of the Class 3 Semaphorins, Front. Cell. Neurosci. 6 (2012) 28. [PubMed: 22783168]

[9]. Hayashi M, Nakashima T, Taniguchi M, Kodama T, Kumanogoh A, Takayanagi H, Osteoprotection by semaphorin 3A, Nature 485 (7396) (2012) 69–74. [PubMed: 22522930]

[10]. Kang S, Kumanogoh A, Semaphorins in bone development, homeostasis, and disease, Semin. Cell Dev. Biol. 24 (3) (2013) 163–171. [PubMed: 23022498]

[11]. Fukuda T, Takeda S, Xu R, Ochi H, Sunamura S, Sato T, Shibata S, Yoshida Y, Gu Z, Kimura A, Ma C, Xu C, Bando W, Fujita K, Shinomiya K, Hirai T, Asou Y, Enomoto M, Okano H, Okawa A, Itoh H, Sema3A regulates bone-mass accrual through sensory innervations, Nature 497 (7450) (2013) 490–493. [PubMed: 23644455]

[12]. Verlinden L, Vanderschueren D, Verstuyf A, Semaphorin signaling in bone, Mol. Cell. Endocrinol. (2015).

[13]. Eisman JA, Bouillon R, Vitamin D: direct effects of vitamin D metabolites on bone: lessons from genetically modified mice, Bonekey. Rep. 3 (2014) 499. [PubMed: 24605216]

[14]. van de Peppel J, van Leeuwen JP, Vitamin D and gene networks in human osteoblasts, Front. Physiol. 5 (2014) 137. [PubMed: 24782782]

[15]. Umesono K, Murakami KK, Thompson CC, Evans RM, Direct repeats as selective response elements for the thyroid hormone, retinoic acid, and vitamin D3 receptors, Cell 65 (7) (1991) 1255–1266. [PubMed: 1648450]

[16]. Heikkinen S, Väisänen S, Pehkonen P, Seuter S, Benes V, Carlberg C, Nuclear hormone 1α,25-dihydroxyvitamin D3 elicits a genome-wide shift in the locations of VDR chromatin occupancy, Nucleic Acids Res. 39 (21) (2011) 9181–9193. [PubMed: 21846776]

[17]. Sutton AL, Zhang X, Dowd DR, Kharode YP, Komm BS, Macdonald PN, Semaphorin 3 B is a 1 25-Dihydroxyvitamin D3-induced gene in osteoblasts that promotes osteoclastogenesis and induces osteopenia in mice, Mol. Endocrinol. 22 (6) (2008) 1370–1381. [PubMed: 18356290]

[18]. Hughes A, Kleine-Albers J, Helfrich MH, Ralston SH, Rogers MJ, A class III semaphorin (Sema3e) inhibits mouse osteoblast migration and decreases osteoclast formation in vitro, Calcif. Tissue Int. 90 (2) (2012) 151–162. [PubMed: 22227882]

[19]. Munetsuna E, Kawanami R, Nishikawa M, Ikeda S, Nakabayashi S, Yasuda K, Ohta M, Kamakura M, Ikushiro S, Sakaki T, Anti-proliferative activity of 25-hydroxyvitamin D3 in human prostate cells, Mol. Cell. Endocrinol. 382 (2) (2014) 960–970. [PubMed: 24291609]

[20]. Nguyen H, Ivanova VS, Kavandi L, Rodriguez GC, Maxwell GL, Syed V, Progesterone and 1,25-dihydroxyvitamin D_3 inhibit endometrial cancer cell growth by upregulating semaphorin 3 B and semaphorin 3F, Mol. Cancer Res. 9 (11) (2011) 1479–1492. [PubMed: 21933904]

[21]. Daci E, Udagawa N, Martin TJ, Bouillon R, Carmeliet G, The role of the plasminogen system in bone resorption in vitro, J. Bone Miner. Res. 14 (6) (1999) 946–952. [PubMed: 10352103]

[22]. Leyssens C, Marien E, Verlinden L, Derua R, Waelkens E, Swinnen JV, Verstuyf A, Remodeling of phospholipid composition in colon cancer cells by 1alpha,25(OH)2D3 and its analogs, J. Steroid Biochem. Mol. Biol. 148 (2015) 172–178. [PubMed: 25625664]

[23]. Meyer MB, Benkusky NA, Lee CH, Pike JW, Genomic determinants of gene regulation by 1 25-dihydroxyvitamin D3 during osteoblast-lineage cell differentiation, J. Biol. Chem. 289 (28) (2014) 19539–19554. [PubMed: 24891508]

[24]. Meyer MB, Benkusky NA, Pike JW, The RUNX2 cistrome in osteoblasts: characterization, down-regulation following differentiation, and relationship to gene expression, J. Biol. Chem. 289 (23) (2014) 16016–16031. [PubMed: 24764292]

[25]. Kent WJ, Sugnet CW, Furey TS, Roskin KM, Pringle TH, Zahler AM, Haussler D, The human genome browser at UCSC, Genome Res. 12 (6) (2002) 996–1006. [PubMed: 12045153]

[26]. Eelen G, Verlinden L, van Camp M, van Hummelen P, Marchal K, de Moor B, Mathieu C, Carmeliet G, Bouillon R, Verstuyf A, The effects of 1alpha 25-dihydroxyvitamin D3 on the expression of DNA replication genes, J. Bone Miner. Res. 19 (1) (2004) 133–146. [PubMed: 14753745]

[27]. Ernst J, Kheradpour P, Mikkelsen TS, Shoresh N, Ward LD, Epstein CB, Zhang X, Wang L, Issner R, Coyne M, Ku M, Durham T, Kellis M, Bernstein BE, Mapping and analysis of chromatin state dynamics in nine human cell types, Nature 473 (7345) (2011) 43–49. [PubMed: 21441907]

[28]. Pundhir S, Bagger FO, Lauridsen FB, Rapin N, Porse BT, Peak-valley-peak pattern of histone modifications delineates active regulatory elements and their directionality, Nucleic Acids Res. 44 (9) (2016) 4037–4051. [PubMed: 27095194]

[29]. Tran TS, Kolodkin AL, Bharadwaj R, Semaphorin regulation of cellular morphology, Annu. Rev. Cell Dev. Biol. 23 (2007) 263–292. [PubMed: 17539753]

[30]. Otsuka E, Yamaguchi A, Hirose S, Hagiwara H, Characterization of osteoblastic differentiation of stromal cell line ST2 that is induced by ascorbic acid, Am. J. Physiol. 277 (1 Pt 1) (1999) C132–138. [PubMed: 10409116]

[31]. Baniwal SK, Shah PK, Shi Y, Haduong JH, Declerck YA, Gabet Y, Frenkel B, Runx2 promotes both osteoblastogenesis and novel osteoclastogenic signals in ST2 mesenchymal progenitor cells, Osteoporos. Int. 23 (4) (2012) 1399–1413. [PubMed: 21881969]

[32]. Verlinden L, Kriebitzsch C, Beullens I, Tan BK, Carmeliet G, Verstuyf A, Nrp2 deficiency leads to trabecular bone loss and is accompanied by enhanced osteoclast and reduced osteoblast numbers, Bone 55 (2) (2013) 465–475. [PubMed: 23598046]

[33]. Sang C, Zhang Y, Chen F, Huang P, Qi J, Wang P, Zhou Q, Kang H, Cao X, Guo L, Tumor necrosis factor alpha suppresses osteogenic differentiation of MSCs by inhibiting semaphorin 3 B via Wnt/b-catenin signaling in estrogen-deficiency induced osteoporosis, Bone 84 (2016) 78–87. [PubMed: 26723579]

[34]. Liu S, Tang W, Fang J, Ren J, Li H, Xiao Z, Quarles LD, Novel regulators of Fgf23 expression and mineralization in Hyp bone, Mol. Endocrinol. 23 (9) (2009) 1505–1518. [PubMed: 19556340]

[35]. Nasarre P, Kusy S, Constantin B, Castellani V, Drabkin HA, Bagnard D, Roche J, Semaphorin SEMA3F has a repulsing activity on breast cancer cells and inhibits E-cadherin-mediated cell adhesion, Neoplasia 7 (2) (2005) 180–189. [PubMed: 15802023]

[36]. Mendes-da-Cruz DA, Brignier AC, Asnafi V, Baleydier F, Messias CV, Lepelletier Y, Bedjaoui N, Renand A, Smaniotto S, Canioni D, Milpied P, Balabanian K, Bousso P, Leprêtre S, Bertrand Y, Dombret H, Ifrah N, Dardenne M, Macintyre E, Savino W, Hermine O, Semaphorin 3F and neuropilin-2 control the migration of human T-cell precursors, PLoS One 9 (7) (2014) e103405.

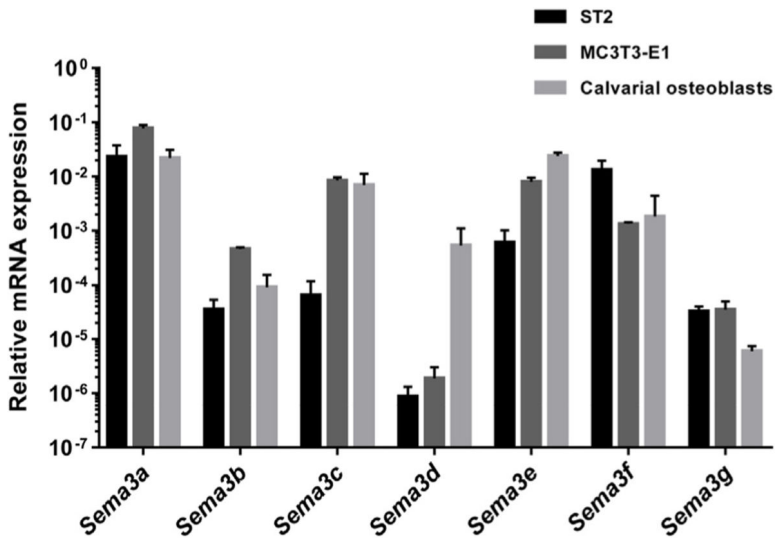

Fig. 1.

Basal mRNA expression levels of semaphorin 3 family members in osteoblastic cells. qPCR was performed to determine the relative basal mRNA expression of *Sema3a*, *3b*, *3c*, *3e*, *3f* and *3g* in ST2 cells (black bars), MC3T3-E1 cells (dark grey bars), and in primary calvarial osteoblasts (light grey bars). Gene expression was analyzed by qPCR in non-treated cells and normalized to the reference gene β-actin. The mean and standard deviation of at least three independent experiments are shown.

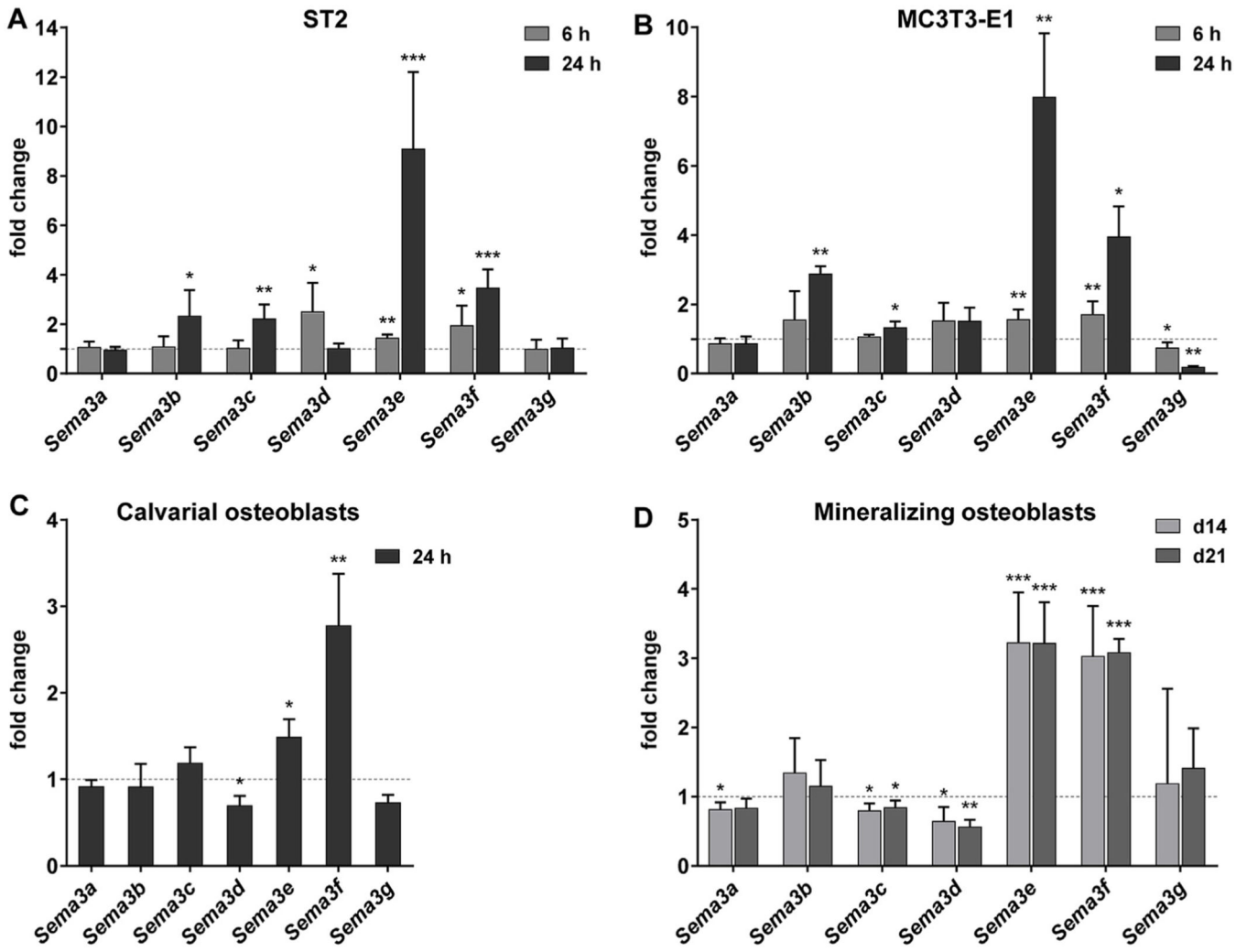

Fig. 2.

Transcript levels of class semaphorin 3 family members were regulated by $1,25(OH)_2D_3$ in osteoblastic cells and during osteoblast mineralization. ST2 (A) and MC3T3-E1 (B) cells were treated with $1,25(OH)_2D_3$ (10^{-8} M) or vehicle for 6 and 24 h. Primary calvarial osteoblasts (C) were treated for 24 h with $1,25(OH)_2D_3$ (10^{-8} M) or vehicle. Cultures of primary calvarial osteoblasts (D) were mineralized 14 or 21 days, and prior to RNA isolation mineralizing cells were treated with $1,25(OH)_2D_3$ (10^{-8} M) or vehicle for 24 h mRNA was isolated and transcript levels of all class 3 semaphorins were analyzed by qPCR. Changes in expression levels by $1,25(OH)_2D_3$ treatment relative to vehicle-treated controls are shown. The mean and standard deviation of at least three independent experiments (A to C), or of merged data from two independent experiments performed in triplicate cultures (D), are shown. One samples *t*-tests were performed to determine the significance of the mRNA induction by $1,25(OH)_2D_3$ (* $p < 0.05$, ** $p < 0.01$, *** $p < 0.001$).

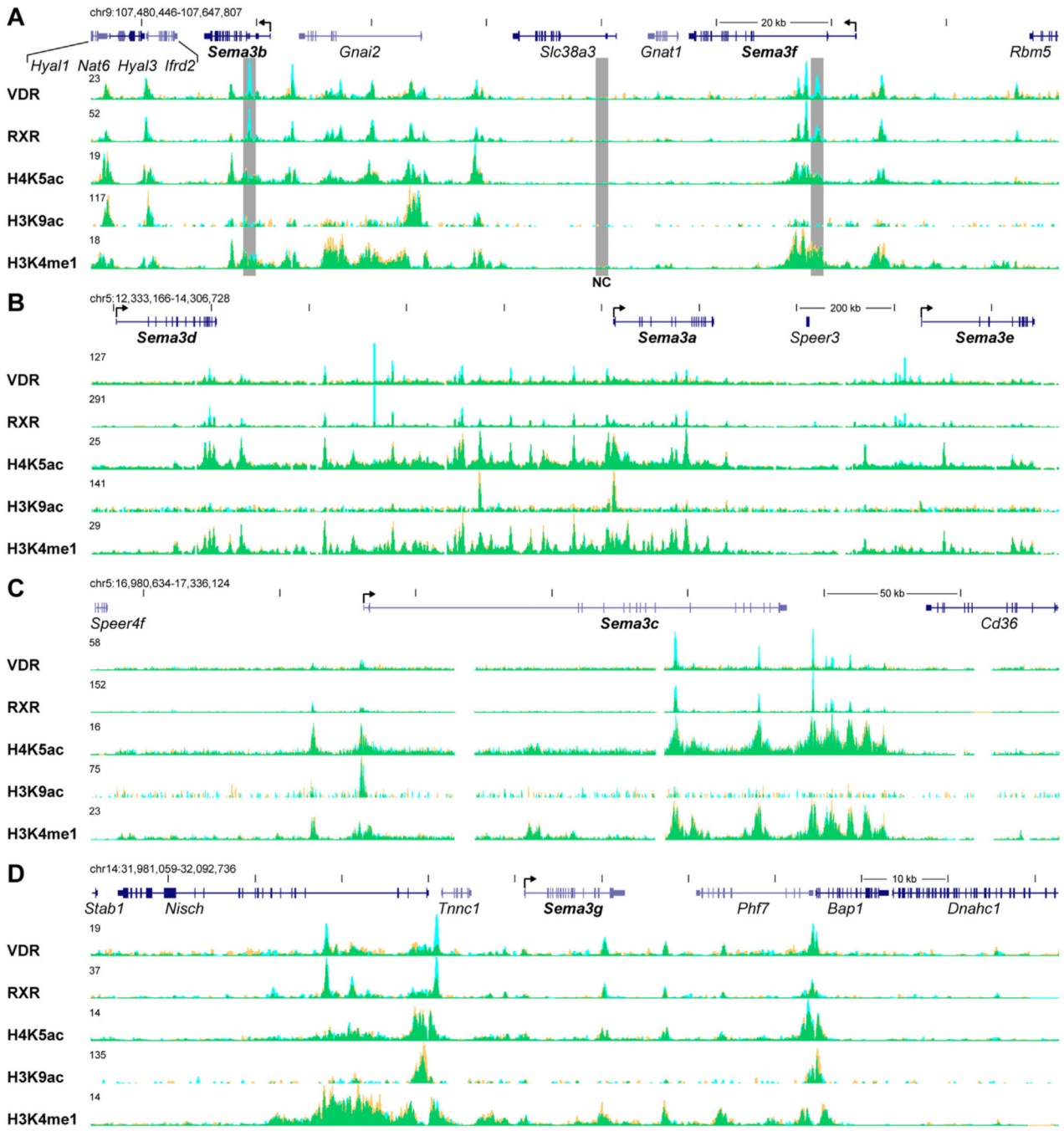

Fig. 3.

VDR and RXR showed direct 1,25(OH)$_2$D$_3$-inducible binding to the genomic regions of *Sema3b* and *3f* genes. Representative ChIP-seq tag density tracks for VDR and RXR binding, and modified histones in vehicle- and 1,25(OH)$_2$D$_3$-treated samples in MC3T3-E1 cells are shown (Veh, yellow; 1,25(OH)$_2$D$_3$, blue; overlap, green). Genomic locations and scales are indicated. Maximum height of tag density for the data track was set according the highest peak of each track and is indicated on the tracks. Genomic regions containing the genes *Sema3b* and *3f* (A), *Sema3d*, *3a*, *3e* (B), *Sema3c* (C) and *Sema3g* (D) are shown.

Transcriptional directions of *Sema3* genes are indicated by an arrow at the TSS. Regions that were further analyzed by ChIP-qPCR are highlighted by gray boxes (NC, negative control).

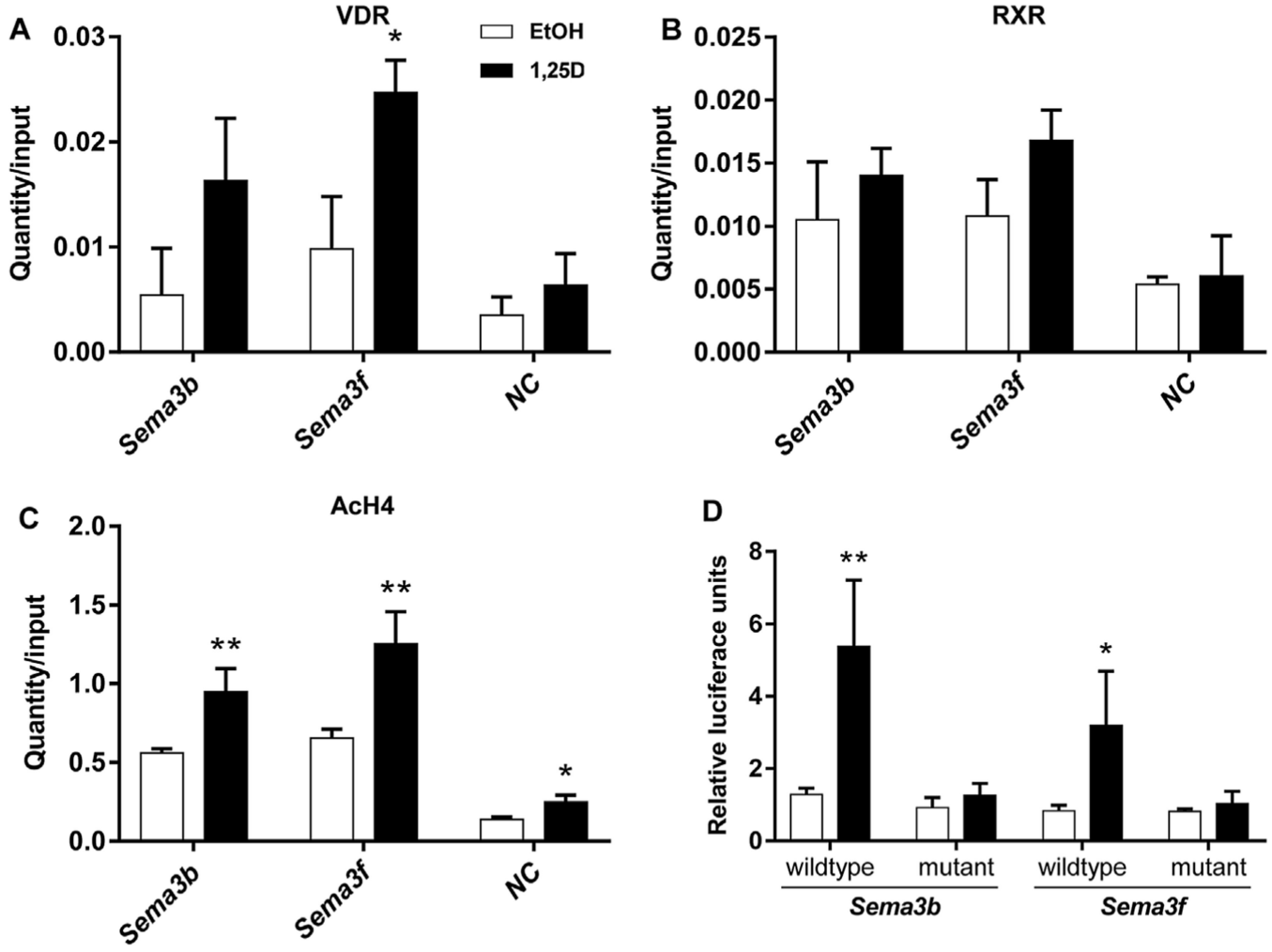

Fig. 4.

ChIP-qPCR and transient transfection assay. ChIP-qPCR results confirmed the ligand-inducible association of VDR (A) and RXR (B), and demonstrated enhanced histone H4 acetylation (C) in response to treatment at the two studied VDR binding sites at genes *Sema3b* and *Sema3f*. ChIP was performed with chromatin samples from MC3T3-E1 cells treated with $1,25(OH)_2D_3$ (10^{-7} M) or vehicle for 3 h. Results show receptor associations and histone H4 acetylation at both binding sites and at NC. The DR3-type VDR binding sites of *Sema3b* and *3f* were further confirmed to be responsive to $1,25(OH)_2D_3$ in transient transfection experiments (D). A DNA fragment, containing either the wildtype or a mutated (non-functional) VDR binding site, was cloned and inserted into the pGL3-Basic vector. Luciferase reporter gene assays were performed to evaluate the functionality of the identified VDR binding sites in exponentially growing MC3T3-E1 cells treated with $1,25(OH)_2D_3$ (10^{-8} M) or vehicle for 24 h. The results were normalized to that of the empty pGL3-Basic luciferase reporter vectors and expressed as means and standard deviations of at least three independent experiments. Two-tailed Student's *t*-tests were performed to determine the significant differences between $1,25(OH)_2D_3$-treated cells and vehicle-treated controls in the

receptor association or chromatin acetylation (A-C), and in the promoter activity (D) (* $p < 0.05$, ** $p < 0.01$).

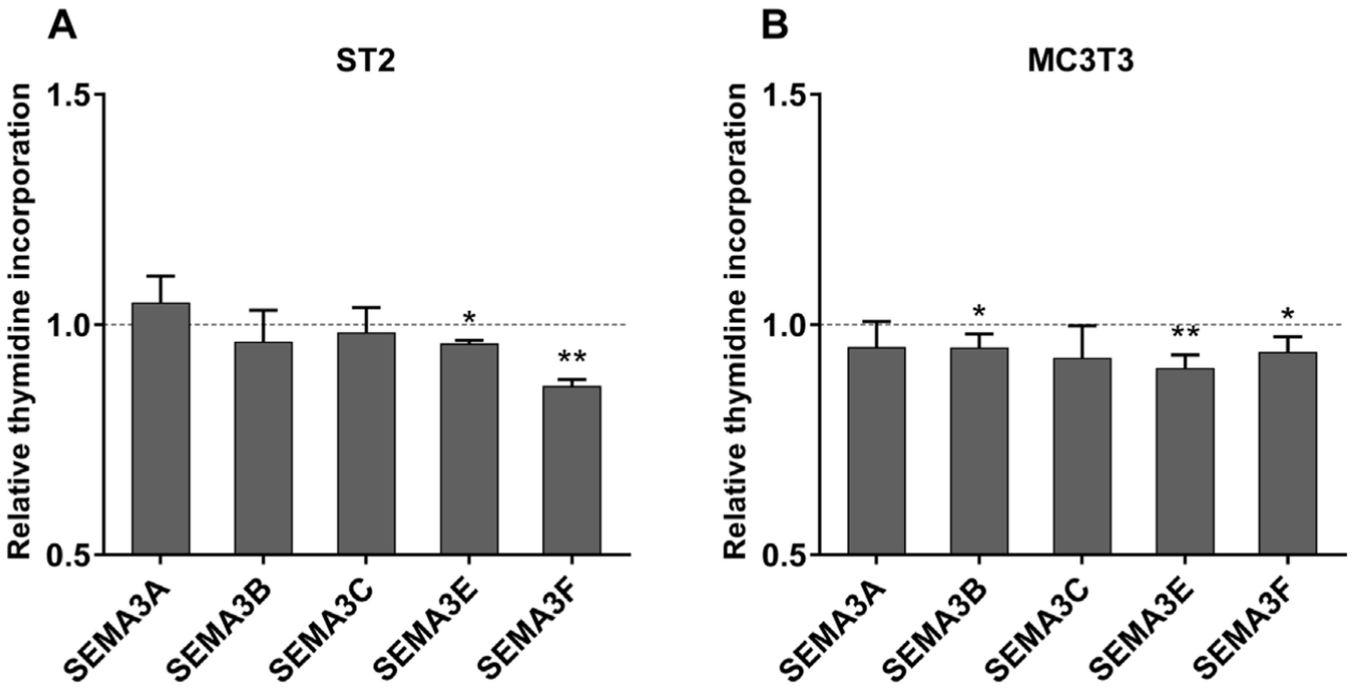

Fig. 5.

ST2 and MC3T3-E1 cell proliferation was reduced by SEMA3E and 3F. ST2 (A) and MC3T3-E1 (B) cells were treated with 640 ng/ml recombinant SEMA3A, 3B, 3C, 3E or 3F protein for 72 h and cell proliferation was evaluated by [^{3}H]thymidine incorporation assay. Changes in thymidine incorporation in SEMA3-treated cells relative to vehicle-treated controls are shown. Data are presented as means and standard deviations of at least three independent experiments. One samples *t*-tests were performed to determine the significance of the inhibition by the treatment (*$p < 0.05$, **$p < 0.01$).

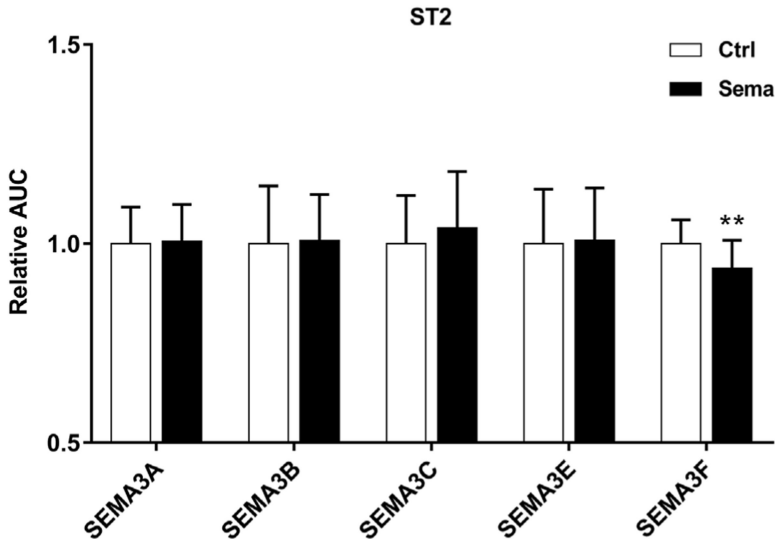

Fig. 6.

SEMA3 treatment did not affect ST2 cell migration in scratch wound assays. Treatment of sub-confluent ST2 cell cultures with recombinant SEMA3A, 3B, 3C, 3E, or 3F protein was started 2 h prior to the introduction of the scratch wound and was continued during the complete experiment. Cell migration was monitored using the IncuCyte ZOOM Scratch Wound assay and an AUC-value was derived for each individual wound as a measure of cell migration (as demonstrated in Fig. S1). Representative experiments performed with 600 ng/ml of SEMA3A, 3B, 3C, 3E, or 3F treatment are shown with results normalized to the mean of the AUC of control wells. Data are presented as means and standard deviations of at least 12 wells. Two-tailed Student's *t*-tests were performed in order to determine the significant differences in cell migration between Sema3-treated cells and vehicle-treated controls (** $p < 0.01$).